[CANCER RESEARCH 64, 7022–7029, October 1, 2004]

A Paracrine Loop between Tumor Cells and Macrophages Is Required for Tumor Cell Migration in Mammary Tumors

Jeffrey Wyckoff,[1] Weigang Wang,[1] Elaine Y. Lin,[2] Yarong Wang,[1] Fiona Pixley,[2] E. Richard Stanley,[2] Thomas Graf,[2] Jeffrey W. Pollard,[2] Jeffrey Segall,[1] and John Condeelis[1]

[1]Departments of Anatomy and Structural Biology and [2]Developmental and Molecular Biology, Albert Einstein College of Medicine, Bronx, New York

ABSTRACT

Invasion of tumor cells into the surrounding connective tissue and blood vessels is a key step in the metastatic spread of breast tumors. Although the presence of macrophages in primary tumors is associated with increased metastatic potential, the mechanistic basis for this observation is unknown. Using a chemotaxis-based *in vivo* invasion assay and multiphoton-based intravital imaging, we show that the interaction between macrophages and tumor cells facilitates the migration of carcinoma cells in the primary tumor. Gradients of either epidermal growth factor (EGF) or colony-stimulating factor 1 (CSF-1) stimulate collection into microneedles of tumor cells and macrophages even though tumor cells express only EGF receptor and macrophages express only CSF-1 receptor. Intravital imaging shows that macrophages and tumor cells migrate toward microneedles containing either EGF or CSF-1. Inhibition of either CSF-1– or EGF-stimulated signaling reduces the migration of both cell types. This work provides the first direct evidence for a synergistic interaction between macrophages and tumor cells during cell migration *in vivo* and indicates a mechanism for how macrophages may contribute to metastasis.

INTRODUCTION

The tumor microenvironment contains stromal cells that influence the behavior of the tumor (1, 2). Of these, there is increasing evidence that macrophages play an important role in modulating the metastatic capacity of the tumor. This includes clinical evidence showing a strong correlation between tumor-associated macrophages (3, 4) and poor prognosis, and genetic studies in mice in which decreased numbers of macrophages in the tumor bed are associated with a large reduction in the rates of metastasis (5, 6). Although macrophages may contribute factors that affect tumor progression by altering the microenvironment with angiogenic and proteolytic factors (6), these cells also are capable of producing growth factors, including members of the epidermal growth factor (EGF) family, which may directly influence the behavior of tumor cells (3, 7). During wound healing or at sites of infection, macrophages synthesize chemotactic factors that recruit other blood cells. Because macrophages migrate to and function within specific tissue sites, it is possible that, within tumors, they also could provide chemotactic cues that promote the egress of carcinoma cells from the tumor (8).

To image and measure migration and chemotaxis at the cellular level within primary metastatic tumors, we have developed animal models that allow direct examination, by intravital imaging, of the behavior of Green Fluorescent Protein (GFP)-expressing carcinoma cells in primary tumors *in vivo* (9–11). Because tumor growth and metastasis are unaffected by expression of GFP (10), the behavioral phenotype of cells within GFP-expressing metastatic and nonmetastatic tumors can be correlated with metastatic potential (11). Intravital imaging of orthotopic rat mammary tumors has shown that increased carcinoma cell orientation and locomotion toward blood vessels correlate with increased numbers of carcinoma cells in blood vessels exiting the primary tumor and with metastasis (9, 11). Growth factors potentially chemotactic for tumor cells including EGF are present in blood, macrophages, platelets, and smooth muscle cells near vessels (12–15). Overexpression of the EGF receptor has been shown to correlate with metastasis and poor prognosis in a number of tumor types, including small-cell lung cancer, breast cancer, gastric cancer, and prostate cancer (16–19). Cell lines that overexpress EGF receptors also are more metastatic *in vivo* (20), and experimental expression of the EGF receptor in nonmetastatic cells increases their chemotactic responses to EGF *in vitro* and metastatic ability *in vivo* (21, 22). Therefore, EGF receptor-mediated chemotaxis within the primary tumor may be important in enhancing invasion, intravasation, and metastasis in addition to the well-characterized effects of EGF receptor signaling on mitogenesis.

We have developed an *in vivo* invasion assay to test the hypothesis that chemotaxis by carcinoma cells in the primary tumor is an important step in invasion. In this assay, cells are collected by chemotaxis from live primary tumors in rats using microneedles filled with Matrigel and containing growth factors to mimic chemotactic signals that may be present in the primary tumor (23). To investigate chemotaxis as a determinant of invasion by carcinoma cells in the primary tumor and the mechanism by which macrophages affect invasion, we have combined the *in vivo* invasion assay with multiphoton-based intravital imaging in mice with mammary tumors produced by the mammary epithelial restricted expression of the Polyomavirus middle T oncogene (PyMT; ref. 24). Transgenic mice selectively expressing PyMT in the mammary epithelium, under control of the mouse mammary tumor virus (MMTV) promoter, rapidly develop multifocal mammary adenocarcinomas (25). Using this approach, we have identified a paracrine interaction involving reciprocal signaling between carcinoma cells and macrophages involving EGF receptor ligands and the macrophage growth factor colony-stimulating factor 1 (CSF-1). This paracrine interaction is involved in the EGF receptor-mediated invasion by carcinoma cells in mammary tumors.

MATERIALS AND METHODS

Mice. Transgenic mice were maintained on a segregating FVB-C3H/B6 background. The details of the origin and identification of *MMTV-PyMT* and *Csf1^{op}/Csf1^{op}/MMTV-PyMT*, *Csf1^{op}/Csf1^{op}/MMTV-PyMT*/CSF-1 TG, *WAP-Cre/CAG-CAT-EGF/MMTV-PyMT*, and *Lys-GFP^{Ki}* mice have been described previously (5, 25–27). *Lys-GFP^{Ki}* mice, in which the insertion of *GFP* into the lysozyme gene locus (*lys-GFP^{Ki}*) created mice with green fluorescent macrophages and granulocytes, were crossed with the *MMTV-PyMT* mice to produce tumors with GFP-labeled macrophages. The *WAP-Cre/CAG-CAT-EGFP* transgene resulted in β-actin promoter-driven eGFP expression that is activated by Cre to label ductal epithelial cells in the mammary gland. Tumors, except when noted, were allowed to grow for 16 to 18 weeks before cell collection to ensure late-stage carcinomas and increased metastasis as described previously (5, 24).

Received 4/26/04; revised 7/14/04; accepted 7/30/04.

Grant support: CA100324 from the National Cancer Institute.

The costs of publication of this article were defrayed in part by the payment of page charges. This article must therefore be hereby marked *advertisement* in accordance with 18 U.S.C. Section 1734 solely to indicate this fact.

Note: Supplementary data for this article can be found at Cancer Research Online (http://cancerres.aacrjournals.org).

Requests for reprints: Jeffrey Wyckoff or John Condeelis, Anatomy and Structural Biology, Analytical Imaging Facility, Albert Einstein College of Medicine, Jack and Pearl Resnick Campus, 1300 Morris Park Avenue, Bronx, NY 10461. Phone: 718-430-3348; E-mail: jwyckoff@aecom.yu.edu or condeeli@aecom.yu.edu.

EGF receptor overexpressing cells were created by transfecting MTLn3 cells using the pLXSN retroviral vector containing the EGF receptor (courtesy of Dr. David Stern, Yale University, New Haven, CT). Cells were selected as a heterogeneous population of G418-resistant clones. Cells were grown in α-MEM with 5% fetal bovine serum (FBS) and harvested using trypsin-EDTA. A total of 1×10^6 cells were injected into the mammary fat pad of severe combined immunodeficiency mice, and tumors were allowed to grow for 4 to 5 weeks before cell collection.

Cell Collection. Cell collection into needles placed into anesthetized animals was carried out as described previously (23, 28). After 4 hours, the collection needles were removed, and the contents were ejected with $\sim$30 μL of L15-BSA through a syringe onto a coverslip. The concentration of growth factors in the needle was determined by multiplying the affinity of the growth factor for its receptor by $\sim$25, which is sufficient to generate a concentration within 100 μm of the bevel of the needle equal to measured concentrations of circulating growth factors *in vivo*.

To inhibit the EGF receptor, PD153035, a tyrosine kinase inhibitor specific for the EGF receptor (29), was used. For inhibiting CSF-1 and the CSF-1 receptor, rabbit antihuman urinary CSF-1 (30) and monoclonal antimouse CSF-1 receptor (ref. 31; courtesy Dr. S. Nishikawa, Kyoto University Medical School, Kyoto, Japan) antibodies were used, respectively. For PD153035, needles were prepared as described previously, containing 10 nmol/L EGF, 25 nmol/L EGF, 25 nmol/L CSF-1, and 10% FBS in L15-BSA with 1% DMSO or 5 μmol/L or 15 μmol/L PD153035 in 1% DMSO. For the antihuman CSF-1 experiments, needles contained 25 nmol/L EGF or 25 nmol/L CSF-1 in L15-BSA with 10 μg of affinity-purified antibody. For the antimouse CSF-1 receptor experiments, needles contained 25 nmol/L EGF or 25 nmol/L CSF-1 in L15-BSA with either 25% nonimmune ascites or 25% antimouse CSF-1 receptor ascites.

To determine whether PD153035 has any effect on CSF-1 receptor-mediated motility, an *in vitro* motility assay was performed. Macrophages were allowed to grow to confluence in three dishes containing DEM without CSF-1 or PD153035, DEM with CSF-1 but no PD153053, or DEM with CSF-1 and 5 μmol/L PD153035. A wound was created, and the cells were imaged on an inverted scope for 7 hours.

Calculation of the Shape of the Gradient Emanating from Collection Needles. The diffusion gradients coming from the needle were estimated by two different methods, assuming diffusion constants of EGF and CSF-1 to be 1.6×10^{-6} cm^2/s (32). In method 1 for the regions immediately inside and outside the needle, linear interpolation, confirmed by relaxation modeling, was used to connect the equations covering the interior and exterior of the needle (33).[3] The results of method 1 were similar to the relaxation model described as method 2 in the Supplemental Data. The results of method 1 are plotted in Fig. 1*E*. The net effects of viscosity in both methods is to change the time scale by a factor corresponding to the increase in viscosity relative to water and could be neglected for the long collection times used in this study.

Multiphoton Imaging of Cell Collection. Cell collection needles were prepared as described previously and placed in *WAP-Cre/CAG-CAT-EGFP/MMTV-PyMT–*, *Tie2-GFP/MMTV-PyMT–*, or *MMTV-PyMT/lys-GFP^{Ki}–*generated primary tumors in an isoflurane-anesthetized mouse placed on an inverted microscope and imaged at 960 nm for GFP fluorescence. *WAP-Cre/CAG-CAT-EGFP/MMTV-PyMT–*generated primary tumors were imaged by multiphoton microscopy performed as described previously (11, 34, 35).

Determination of Cell Types Collected. Cells collected into needles were extruded into a poly-L-lysine–coated MatTek dish (MatTek Corp., Ashland, MA) containing 20 μL of 10% paraformaldehyde and fixed for 30 minutes. Nonspecific binding was blocked with 100 μL Tris-buffered saline (TBS) with 1% FBS overnight at 4°C. The blocking solution was removed, and a primary antibody mixture of rabbit anti-pankeratin for carcinoma cells and rat anti-F4/80 (36) for macrophages was added in TBS with 1%BSA (TBS-BSA) for 1 hour at room temperature. The cells were rinsed three times with TBS-BSA and incubated in a mixture of goat antirabbit Cy3 and sheep antirat FITC secondary antibodies in TBS-BSA for 1 hour at room temperature. The cells were rinsed as described previously and left in TBS-BSA; 4′,6-diamidino-2-phenylindole (DAPI) was added; and the cells were counted.

[3] Berg, personal communication.

Real Time-PCR. Quantitative real time-PCR analysis of mRNA was performed with sequence-specific primer pairs for different cell type markers. Keratin 18 is a type I intermediate filament protein that is expressed in nearly all of the epithelial malignancies. Mac-1 is a macrophage antigen. For the paracrine loop components, mRNA was extracted from fluorescence-activated cell-sorted (FACS) carcinoma cells and FACS macrophages from primary tumors originating in *WAP-Cre/CAG-CAT-EGFP/MMTV-PyMT* mice and used with sequence-specific primer pairs for the EGF receptor, EGF, CSF-1, and the CSF-1 receptor. Carcinoma cells were sorted by their GFP fluorescence using FACS, whereas macrophages were sorted using the F4/80 primary antibody and R-phycoerythrin–labeled antirat secondary antibody (PharMingen, San Diego, CA). Experiments were performed by following standard procedures described previously (11).

RESULTS

Growth Factor Specificity of Cell Collection. We used *MMTV-PyMT*–induced mammary tumors in mice (25) and the *in vivo* invasion assay described previously (23) to study chemotaxis by carcinoma and host cells within live primary tumors. Initially EGF was used to visualize the migration of chemotactic cells. Using multiphoton microscopy, the collection of carcinoma cells and macrophages into microneedles in the living tumor was observed directly by time-lapse imaging (Fig. 1*A* and *B*). Mice with *PyMT* tumors resulting from crosses of either *MMTV-PyMT/WAP-Cre/CAG-CAT-EGFP* (GFP-expressing carcinoma cells; ref. 26) or *MMTV-PyMT/lys-GFP* mice (GFP-expressing macrophages; ref. 27) were used. In these animals, macrophages and carcinoma cells were observed to actively move toward collecting needles filled with EGF at velocities of several micrometers per minute for both cell types.

Chemotaxis was analyzed in response to a variety of growth factors reported to be involved in progression to malignancy. The growth factors used were chosen for the following reasons: EGF receptor expression is correlated with poor prognosis in breast cancer, and EGF and transforming growth factor α (TGF-α) are chemotactic for breast carcinoma cells (37–39). CSF-1 and CSF-1 receptor expression is correlated with invasive mammary tumors in human populations and animal models (40, 41), and CSF-1 is chemotactic for macrophages (38, 42) Heregulin has been shown to enhance motility and migration of cancer cells (43) and, as the ligand for the ErbB2/ErbB3 heterodimer, has been shown to enhance cell proliferation in breast cancers (44). Platelet-derived growth factor (PDGF) B/B is produced by macrophages and stimulates cell motility in connective tissue cells, monocytes, and neutrophils (45) and is correlated with invasion in a number of human cancers (46). Furthermore, PDGF receptor β, which responds to PDGF B/B, is found on monocytes and macrophages (47, 48). Vascular endothelial growth factor α (VEGF-α) is correlated with angiogenic response (49) and has been shown to stimulate invasion in breast cancer cells (50). FGF-1 also has been shown to induce malignant behavior in breast cancer (51).

The most efficient cell collection occurred in response to EGF and TGF-α, and CSF-1 (Fig. 1*C*). FBS, which contains several of the growth factors used in Fig. 1*C*, also was effective in collecting cells. This collection was inhibited with PD153035, an inhibitor of the EGF receptor, and was therefore EGF receptor dependent. Heregulin, VEGF-α, FGF-1, and PDGF B/B were not effective at collecting cells above levels obtained with buffer alone.

Cell collection into microneedles filled with various concentrations of EGF, TGF-α, and CSF-1 followed reproducible dose-response curves in *MMTV-PyMT*–derived tumors (Fig. 1*D*). Approximately 1000 cells were collected from primary tumors of 18-week-old wild-type *MMTV-PyMT* animals in each needle in 4 hours at the optimum concentration of each EGF receptor ligand and CSF-1, whereas no cells above background were collected with the same range of con-

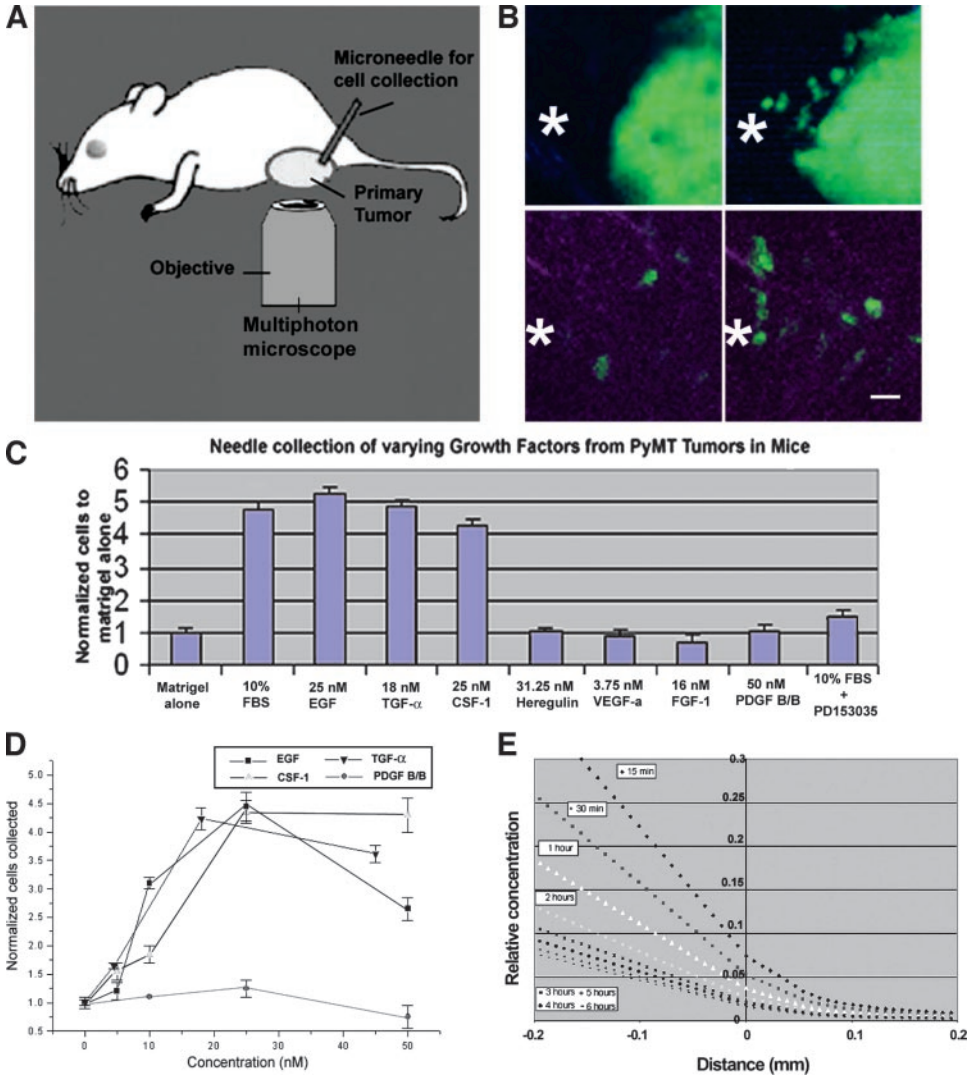

Fig. 1. Movement of macrophages and carcinoma cells into collection needles in response to growth factors. *A*, Model shows how the experiment is performed. The primary tumor in the right number 5 mammary gland is selected to minimize breathing motion, and the position of the collection needle is controlled with a micromanipulator (not shown). *B*, movement of fluorescent carcinoma cells (*top*, *WAP-Cre/CAG-CAT-EGFP/MMTV-PyMT* tumor) and macrophages (*bottom*, *MMTV-PyMT/lys-GFP^{Ki}* tumor) toward EGF-containing collecting needles. ∗, The approximate opening of the collection needle is shown in each field. Each image is a 50-μm z-projection and is from a time-lapse series. Images on the right were recorded 90 minutes after images on the left; *bar*, 25 μm. *C*, Collections (4 hours each) of cells from PyMT-generated tumors using various growth factors show effects for FBS and EGF, TGF-α, and CSF-1 receptors. Collection by FBS is inhibited by PD153035. Similar results were obtained for other collection times. *D*, Dose-response curves for EGF, TGF-α, and CSF-1 show maxima for cell collection, whereas PDGF failed to collect cells above background. Concentration refers to the concentration in the needle. *E*, The growth factor concentration delivered various distances from the needle tip, with 0 = to the center of the bevel of the needle, was calculated according to diffusion for 25 nmol/L EGF or CSF-1 placed inside the needle. Y-axis is the fraction of 25 nmol/L at the time and position indicated after insertion of the needle into the tumor. Diffusion predicts 0.2 to 1.3 nmol/L free growth factor concentrations 100 μm from the edge of the needle during the collection time interval used for the experiments reported in this article.

centrations of the other growth factors (Fig. 1*C* and *D*). Unlike CSF-1, TGF-α did not show up on array analysis as being up-regulated in invasive carcinoma cells collected using the *in vivo* invasion assay (data not shown); therefore, it was not investigated further.

The concentrations given in Figs. 1 and 2 are those loaded within the collection needles. The concentration of the growth factor delivered within 100 μm of the opening of the needle containing 25 nmol/L ligand, a place where cell migration in response to the needle was observed by multiphoton imaging (Fig. 1*B*), was calculated based on diffusion in a low Reynolds number environment, such as whole tissue, to be ~0.2 to 1.3 nmol/L (Fig. 1*E* and Materials and Methods). The circulating concentrations for these growth factors *in vivo* are reported to be 0.18 to 1.5 nmol/L, suggesting that cells near the collection needle were responding to physiologic concentrations of these growth factors (52, 53).

To determine whether cell collection efficiency was related to EGF receptor expression, the collection of cells was scored from mammary tumors made by injecting carcinoma (MTLn3) cells, overexpressing the EGF receptor, into the mammary fat pads of severe combined immunodeficiency mice. Overexpression of EGF receptor caused a significant increase in the number of carcinoma cells collected from mammary tumors at both concentrations of EGF tested (Fig. 2*A*). These results are consistent with previous studies in which cell lines expressing low levels of EGF receptor generated tumors from which only background levels of cells were collected, indicating a contribution of the EGF receptor to cell collection (23).

Macrophages were collected from the mammary tumors in response to either EGF or CSF-1 (Fig. 2*B*) and were observed by multiphoton imaging directly during collection in *lys-GFP^{Ki}* mice with tumors (Fig. 1). In response to PDGF, however, the number of cells collected was at the level of the buffer background (~150 cells), and few were macrophages based on imaging of GFP-macrophages (Fig. 2*B*). When needles were placed into normal mammary fat pads of similarly aged *lys-GFP^{Ki}* mice, only ~20 cells were collected in response to CSF-1,

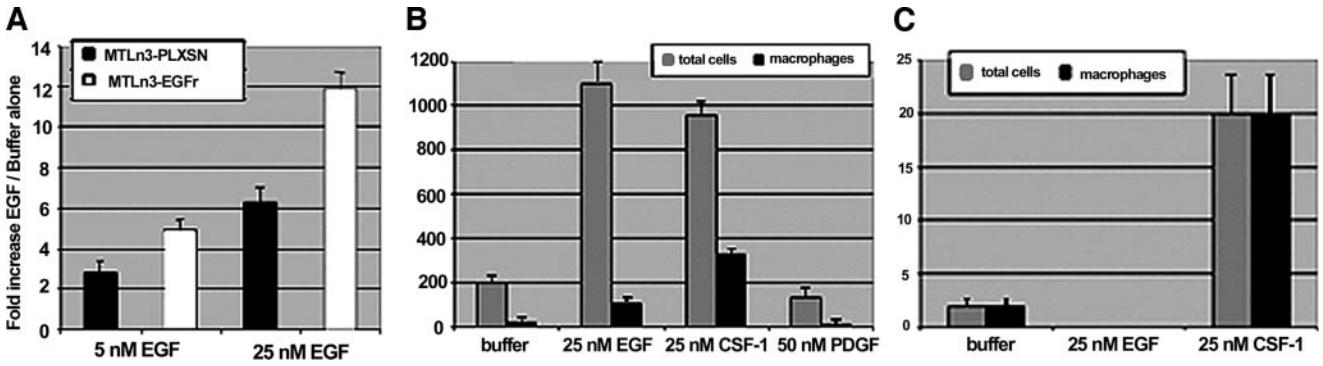

Fig. 2. Characterization of cell collection with microneedles from mammary tumors. *A*, Cells were collected in higher numbers (3-hour collection interval is shown) from tumors prepared with carcinoma (MTLn3) cells overexpressing the EGF receptor than from tumors prepared with MTLn3 cells transfected with empty vector (pLXSN). Each cell type was collected from three tumors with two needles for each experiment. *B*, example of collection of cells from *MMTV-PyMT/lys-GFP*^{Ki} tumors in 18-week-old tumors. Cells were scored by staining them with DAPI to count all of the cells present and by GFP expression for macrophages. In needles containing 50 nmol/L PDGF, only background numbers of cells were collected (buffer = the number collected in the needle containing Matrigel alone). *C*, Few cells were collected from the *lys-GFP*^{Ki} normal mammary gland and only in response to CSF-1, and all were macrophages as confirmed by GFP fluorescence (buffer = Matrigel alone; $n = 3$, ±SE for *A–C*).

and all were GFP labeled, suggesting a greatly decreased response exclusively by macrophages (Fig. 2*C*). During the same collection time interval, a mixture of >1000 carcinoma cells and macrophages was collected from mammary tumors (compare scales in Fig. 2*B* and *C*).

Only Macrophages and Carcinoma Cells Migrate into Needles. To determine the cell types collected from PyMT mouse mammary tumors into EGF- and CSF-1–containing needles with more precision, DAPI stain was used for all of the cells, anti-pankeratin was used for carcinoma cells, and anti-F4/80 was used for macrophages. F4/80 is a macrophage lineage restricted antigen and is not found on neutrophils (36), although it is found on eosinophils, which can be easily distinguishable by morphology (54). As shown in Fig. 3*A*, in response to EGF, carcinoma cells comprised ~73% of the cell population collected, whereas macrophages comprised 26%, collectively accounting for >99% of the cells collected. Similar results were obtained with CSF-1–containing needles (not shown). Furthermore, the same results were obtained with another animal model with mammary tumors in rats prepared by injecting cultured carcinoma cells (MTLn3) into the mammary fat pads (Fig. 3*B*). Cell collection from the rat tumors showed that carcinoma cells comprised 76% and macrophages accounted for 23% of collected cells (Fig. 3*B*). These results indicate that the comigration of macrophages and carcinoma cells is a common property of mammary tumors in different animal models regardless of how the primary tumor was formed and may reveal a common underlying mechanism for migration and possibly invasion.

Quantitative real time-PCR was used to determine the relative enrichment of macrophages and carcinoma cells in the microneedles relative to the primary tumor using macrophage (MAC-1) and carcinoma cell (keratin)-specific primers. mRNA was isolated from the cells collected in the microneedles with 25 nmol/L EGF (Fig. 3*C*). The results show a sixfold enrichment of macrophages (*MAC-1* gene) over that found in the primary tumor, whereas the carcinoma cells were not significantly enriched. Quantitative real time-PCR of pieces of tissue obtained from needle biopsies of the same tumor showed no enrichment for macrophages (Fig. 3*C*), indicating that the macrophages in EGF and CSF-1 microneedles were actively collected by chemotaxis and not passively collected by punching the needle into the tumor as in the biopsy. This is consistent with observations made during multiphoton imaging, in which active motility of cells toward the collection needles was observed (Fig. 1*B*).

To investigate why macrophages and carcinoma cells are collected by needles containing either EGF or CSF-1, the expression pattern of these growth factors and their receptors in tumor-associated macrophages and carcinoma cells was determined by real time-PCR. As shown in Fig. 4, carcinoma cells isolated from *WAP-Cre/CAG-CAT-EGFP/MMTV-PyMT*–generated primary tumors by FACS express EGF receptor and CSF-1 but neither EGF nor CSF-1 receptor. The GFP-labeled carcinoma cells also were shown to express the PyMT antigen by real time-PCR (Fig. 4*A*), and the carcinoma cells also stained positively for the PyMT antigen in histologic sections (Fig. 4*B*). The reciprocal pattern of expression in FACS macrophages from the same tumor was observed. The macrophages expressed CSF-1

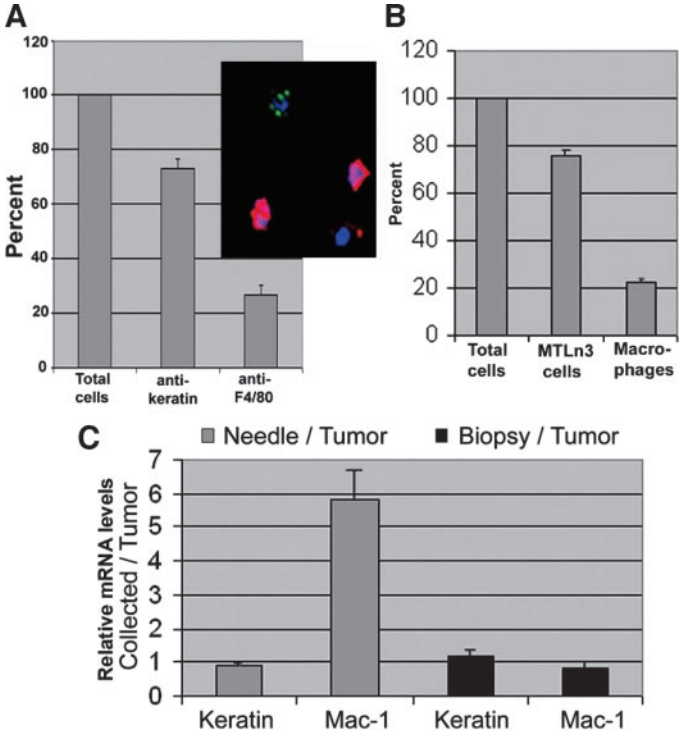

Fig. 3. Macrophages and carcinoma cells are selectively collected from the primary tumor with EGF-containing microneedles. *A*, counts of cell types from a typical needle, for which DAPI is a marker for total cells, antikeratin is a marker for carcinoma cells, and anti-F4/80 is a marker for macrophages. Inset shows cells from a needle after staining, where carcinoma cells are red, macrophages are green, and DAPI is blue. The proportion for macrophages differs from those in Fig. 2 because GFP expression measured in Fig. 2 is not uniform in all of the macrophages, leading to an underestimation of macrophage number. *B*, counts of cell types from MTLn3-induced mammary tumors of rats scored as described in *A*. *C*, Quantitative real time-PCR using primers specific for keratin 18 (carcinoma cells) and MAC-1 (macrophages) is shown for RNA from cells collected into needles by chemotaxis and from a needle biopsy ($n = 3$, ±SE for *A* and *B*).

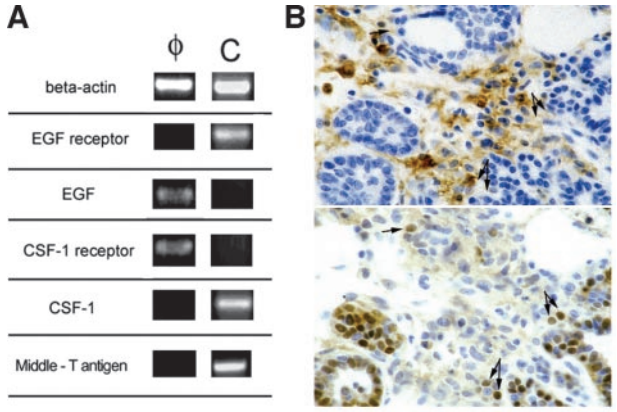

Fig. 4. The relationship between carcinoma cells and macrophages in mammary tumors. *A*, carcinoma cells (C) isolated from primary mammary tumors by FACS express EGF receptor and CSF-1 but neither EGF nor CSF-1 receptor mRNA by PCR. The pattern of expression in the FACS tumor-associated macrophages (ϕ) is the opposite of the carcinoma cells, showing mRNA expression of CSF-1 receptor and EGF but not for the EGF receptor or CSF-1. Only carcinoma cells express the middle T antigen. *B*, immunohistologic staining of adjacent sections of a tumor for macrophages (*top*) with F4/80 antibodies and carcinoma cells (*bottom*) with anti-PyMT antibodies. Invading carcinoma cells (*bottom*, *arrows*) are seen in the stroma adjacent to macrophages (*top*) in an invasive area. Arrows indicate the positions of the carcinoma cells.

receptor and EGF but not CSF-1, EGF receptor, or the PyMT antigen (Fig. 4*A*). CSF-1 radioimmunoassays (30) of extracts of tumors at different stages showed that small tumors with more stromal cells than carcinoma cells had undetectable levels of CSF-1, whereas large tumors that consisted of mainly carcinoma cells had modest levels of CSF-1 (not shown; ref. 5). This, along with the real time-PCR data, indicates that the carcinoma cells produce CSF-1.

The PCR results are consistent with *in situ* hybridization results showing that macrophages are the only cells adjacent to carcinoma cells in *PyMT*-derived tumors that express the CSF-1 receptor (5). Immunostaining using anti–F-4/80 for macrophages and anti–middle-T antigen for carcinoma cells shows that macrophages are found near carcinoma cells in the invasive margin of the mammary tumor in histologic sections (Fig. 4*B*). Our results raise the interesting possibility that carcinoma cells and macrophages are engaged in a paracrine interaction causing them to move as coupled cells toward a source of either EGF or CSF-1. Other cell types that express the EGF receptor, such as fibroblasts (55, 56) and vascular endothelial cells (57), were not collected in the needles, possibly because they do not enter either an autocrine- or paracrine-mediated amplification of the chemotactic signal by secreting chemotactic cytokines in response to exogenous EGF stimulation.

Macrophages Are Required for Carcinoma Cell Migration in Response to EGF and CSF-1. In transgenic mice susceptible to mammary cancer (MMTV-*PyMT* mice) that also are homozygous for the *Csf1*^{op} allele (CSF-1 deficient), neither the incidence nor the growth of primary tumors is affected by the absence of CSF-1. However, these mice have a low density of tissue macrophages because of the chronic absence of CSF-1 (58). This is correlated with delayed onset of metastasis (5). To investigate the importance of macrophages in carcinoma cell migration, cell collection in microneedles from *PyMT*-generated tumors in a *Csf1*^{op}/*Csf1*^{op} background was compared with cell collection from tumors in wild-type mice (Fig. 5*A*). Here we show a large reduction in the collection of cells from mammary tumors in the *Csf1*^{op}/*Csf1*^{op} background by needles filled with either EGF or CSF-1 as compared with cells collected from wild-type *PyMT* tumors (Fig. 5*A*). Macrophages comprised 5 to 7% of the population of cells collected from the *PyMT*-generated tumors in the *Csf1*^{op}/*Csf1*^{op} background mice using a needle containing 25 nmol/L EGF, consistent with low macrophage densities in the *Csf1*^{op}/*Csf1*^{op} tumors. These results indicate that the chemotactic and migratory responses of carcinoma cells to EGF depend on the presence of macrophages.

To directly test the requirement for CSF-1 in invasion, 18-week-old tumors in *Csf1*^{op}/*Csf1*^{op}/*PyMT* CSF-1 TG mice, which contain the MMTV-driven *CSF-1* transgene, were used. The *CSF-1* transgene only expresses CSF-1 in the mammary and salivary gland because of the MMTV promoter and causes the acceleration of tumor progression and metastasis (5, 53). In these animals, 1.7-fold more carcinoma cells were collected in needles containing 25 nmol/L EGF than from similar aged *Csf1*^{op}/*Csf1*^{op}/*PyMT* tumors (Fig. 5*B*). These results indicate that expression of CSF-1 in the mammary gland potentiates the migration of carcinoma cells in response to EGF.

To further investigate the relationship between macrophages and the collection of carcinoma cells by chemotaxis, CSF-1 was infused

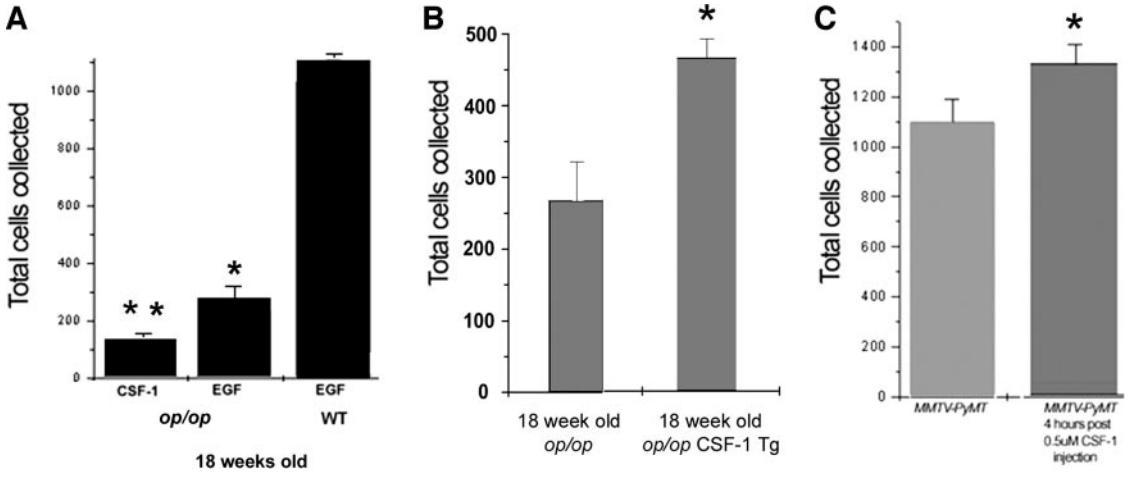

Fig. 5. Collection of invasive cells into needles is tumor stage specific and delayed in *Csf1*^{op}/*Csf1*^{op}× *PyMT* tumors. *A*, The number of macrophages and carcinoma cells collected in needles from CSF-1–deficient *Csf1*^{op}/*Csf1*^{op}/*PyMT* mammary tumors was greatly decreased in CSF-1– and EGF-containing needles compared with wild type (wt) at 18 weeks. This is consistent with the low invasive and metastatic potential of PyMT tumors in the *op/op* genetic background (*, statistically significant differences between EGF collections of *Csf1*^{op}/*Csf1*^{op} and wild-type tumors, $P < 0.001$; **, statistically significant differences between CSF-1 collections of *Csf1*^{op}/*Csf1*^{op} and wild-type tumors, not shown; compare with Fig. 2*B* tumors; $P < 0.002$; $n = 3$, ±SE). *B*, Cell collection from 25 nmol/L EGF-containing needles in 18-week-old *Csf1*^{op}/*Csf1*^{op}/*PyMT* CSF-1 TG tumors showed a 1.7-fold increase over *Csf1*^{op}/*Csf1*^{op}× *PyMT* tumors of the same age (*, $P < 0.024$). *C*, Preinjection of 0.5 μmol/L CSF-1 into a *PyMT* mouse mammary tumor 4 hours before the start of needle collection increased the collection of cells from the same tumor. In needles containing 25 nmol/L EGF, a 16% increase in the number of cells collected was seen in tumors preinjected with CSF-1 compared with controls (*, significant differences from control mock injected mice, $P < 0.034$).

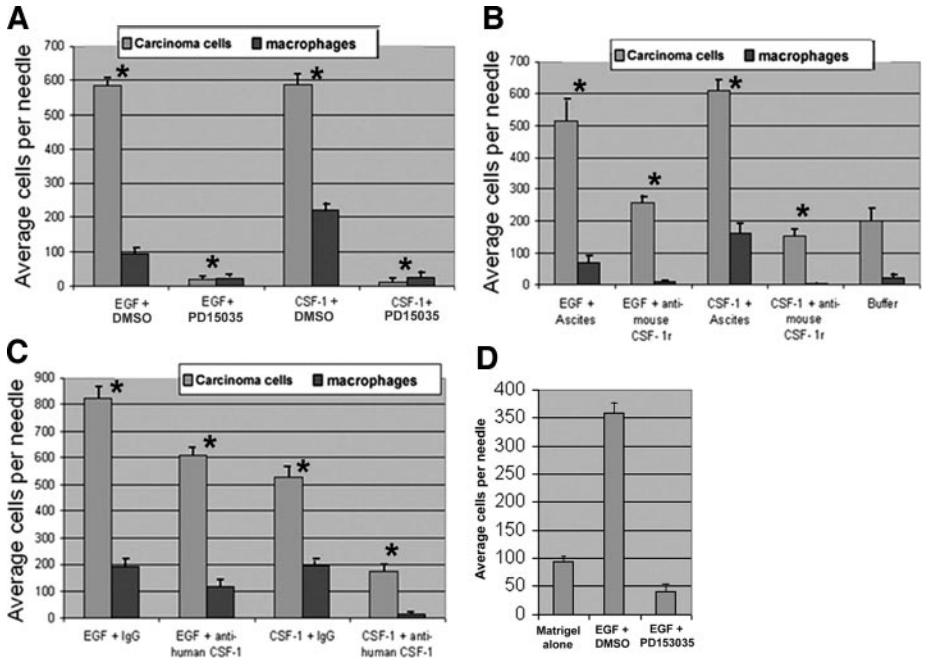

Fig. 6. Cell collection into microneedles is inhibited by blocking the function of either EGF receptor or CSF-1 receptor. *A*, Inhibition of cell collection into needles containing 10 nmol/L EGF or 25 nmol/L CSF-1 by the EGF receptor inhibitor PD153035 at 15 μmol/L is shown (*, for both conditions, $P < 0.0008$ comparing $\pm$ PD153035). Other experiments not shown are in needles containing 25 nmol/L EGF; 5 μmol/L and 15 ìmol/L PD153035 reduced the number of cells collected by ~50%. When the concentration of EGF was decreased to 10 nmol/L in the needle, the number of cells collected decreased below the background level. In needles containing 25 nmol/L human CSF-1, 5 μmol/L PD153035 reduced cell collection to well below background. *B*, inhibition of cell collection into needles containing 25 nmol/L growth factor by antimouse CSF-1 receptor (*, for both conditions, $P < 0.0015$ comparing $\pm$ antibody). *C*, Cell collection into needles containing 25 nmol/L growth factor is significantly inhibited by anti-human CSF-1 in human CSF-1–containing microneedles but only partially in EGF-containing microneedles (*, for EGF, $P < 0.006$ and for CSF-1, $P < 0.0003$ comparing $\pm$ antibody; $n = 3$, $\pm$SE for *A–C*). *D*, inhibition of cell migration into needles containing 10 nmol/L EGF from MTLn3-induced mammary tumors of the rat by the EGF receptor inhibitor PD153035 at 15 μmol/L ($P < 0$ 0.0006 comparing $\pm$ PD153035).

locally into the *MMTV-PyMT* tumor 4 hours before needle collection. CSF-1 has been shown to recruit macrophages to the point of administration in the pleural and peritoneal cavities (59). Previous introduction of CSF-1 into the tumor significantly increased the collection of cells into microneedles containing EGF (Fig. 5*C*). The cells collected into an EGF-containing needle after injection of CSF-1 into the tumor showed a similar ratio of carcinoma cells to macrophages as noninjected tumors (72% to 27%), indicating the enhanced collection of carcinoma cells and macrophages in response to priming the tumor with just CSF-1. These results suggest that the presence of macrophages is essential for the full chemotactic potential of carcinoma cells to be realized in *PyMT* tumors during cell collection by microneedles.

Requirement of EGF- and CSF-1–Mediated Signals for Cell Migration. Our results suggest the presence of a paracrine loop in which the carcinoma cells are a source of CSF-1, which attracts macrophages, whereas macrophages respond by releasing EGF, which stimulates carcinoma cells. To further investigate the existence of a paracrine loop, PD153035, a tyrosine kinase inhibitor specific for the EGF receptor (29), and antibodies that block CSF-1 receptor activity were added to the collection needles to investigate the relative contributions of these growth factor receptors to cell migration in *PyMT* tumors of 18-week-old wild-type mice. PD153035 is reported to have no effect on the activity of CSF-1 receptor (29). PD153035 also had no effect on the motility of BAC1.2F5 macrophages in response to CSF-1 *in vitro* (data not shown). The addition of PD153035 to needles containing EGF or CSF-1 inhibited cell collection (Fig. 6*A*). In CSF-1–containing needles, the number of macrophages collected from tumors in the presence of PD153035 was similar to that collected from normal tissue in response to CSF-1 (Fig. 2*C*), consistent with *in vitro* results showing that PD153035 does not inhibit macrophage motility. Similar inhibitory results with PD153035 were obtained with an independent animal model (described in Fig. 3*B*) using rats with mammary tumors derived from injection of MTLn3 cells (Fig. 6*D*).

Addition of antibodies to needles that block the activity of murine CSF-1 receptor also resulted in the inhibition of cell collection in EGF- and CSF-1–containing needles to background levels (Fig. 6*B*). The percentage of cells that were macrophages in EGF and CSF-1 needles decreased to <3%, indicating the macrophage motility requires CSF-1 receptor activity.

The addition of antibodies to needles that block human but not mouse CSF-1 resulted in only a slight inhibition of EGF-mediated collection of cells, indicating an endogenous source of mouse CSF-1 during collection. Inhibition to background levels of cell collection was observed in needles containing human CSF-1 and its antibody as expected (Fig. 6*C*). These results are consistent with the ability of the antihuman CSF-1 antibody to inhibit only human CSF-1 placed in the needle and not the mouse CSF-1 generated *in situ* in response to EGF.

In aggregate, these experiments indicate that the activities of the receptors for EGF and CSF-1 contribute to the collection of carcinoma cells and macrophages from mammary tumors in these two independent animal models in response to either EGF or CSF-1, consistent with the presence of a paracrine loop.

DISCUSSION

We have shown that in mammary tumors derived from the expression of the *PyMT* oncogene in mice and in rats and severe combined immunodeficiency mice injected orthotopically with carcinoma cell lines, a paracrine loop operates involving the interaction of carcinoma cells and macrophages. In mouse mammary tumors, in response to needles containing either EGF or CSF-1, only carcinoma cells and macrophages are collected. This is a true paracrine loop requiring the activity of the EGF and CSF-1 receptors on separate cell types because CSF-1 receptors are expressed only on macrophages and EGF receptors are expressed only on carcinoma cells, and inhibition of collection of both cell types results from inhibition of either receptor type. These data, along with the studies described previously (5), support the existence of a paracrine loop involving the mutual signaling and chemotaxis between macrophages and carcinoma cells that is essential for motility and invasion in mammary tumors. The use of either CSF-1 or EGF in the collection needle may mimic a process in which CSF-1 secreted by carcinoma cells leads to the activation of macrophages to secrete EGF receptor ligands, leading to stimulation of carcinoma cell movement.

The paracrine loop described in this study may be related to

malignancy because (1) few cells are collected into needles placed into normal mouse mammary fat pads; (2) the collection of cells from *Csf1^{op}/Csf1^{op}/PyMT* mice is carcinoma stage specific and follows the delay in progression to malignancy because of the absence of endogenous CSF-1 and a low density of tissue macrophages (5); and (3) in recent studies involving one of us (E.R.S), it was shown that mouse CSF-1 antisense administered to nude mice bearing human colon cancer xenografts decreased CSF-1 protein expression and increased mouse survival (60). More recently, the same group has shown that mouse CSF-1 blockade by antisense oligonucleotides or small interfering RNAs suppressed the growth of human mammary tumor xenografts in nude mice and improved mouse survival. These treatments also suppressed host macrophage infiltration within tumors (61).

The novelty of our results is the direct demonstration of the existence of a robust and self-propagating paracrine loop in mammary tumors and demonstration of the mechanism by which macrophages enhance carcinoma cell migration by completing this paracrine loop. Macrophages have been hypothesized to play a role in tumor rejection and increased malignancy (3, 4, 62). These opposing hypothetical roles have kept the importance of tumor-associated macrophages in tumor invasion controversial. Our results define a role for macrophages in enhancing cell migration that could contribute to invasion and metastasis. They also suggest a model to explain the requirement for CSF-1 in invasion and progression to metastasis seen in studies with CSF-1–deficient mice (5).

The chemotaxis of cells that move slowly compared with the rate of diffusion of chemoattractant generally requires the renewed propagation of the chemotactic signal from cell to cell to retain a steep gradient of chemoattractant near each responding cell (63). The classic example of this type of chemotaxis is that exhibited by *Dictyostelium* amoebae during mound formation, in which large fields of cells are attracted by the relay of cyclic AMP from cell to cell throughout a large aggregation field (64). The result is the recruitment of hundreds of thousands of cells from 1 million μm^2 of area during morphogenesis, a scale of cell collection that would not be possible by simple diffusion from a point source. In the absence of the ability to relay the chemotactic signal, only cells immediately adjacent to the founder cell, the cell that initially secretes cyclic AMP, would respond, and mound formation would fail. We propose that autocrine and paracrine loops exist in tumors that achieve the same relayed chemotaxis effect by recruiting cells from volumes of the tumor that are vast compared with that possible by simple diffusion of chemoattractant alone. This hypothesis predicts that every malignant tumor has a well-developed aggregation field using defined chemoattractants to drive autocrine and/or paracrine loops, resulting in the accumulation of cells around the initiating chemotactic signal. It is possible that autocrine and paracrine loops will be tumor type specific and will operate not only in the primary tumor but also in secondary and tertiary metastatic tumors. The ability to disrupt autocrine- and paracrine-based relayed chemotaxis raises the possibility that the discovery of self-propagating chemotaxis loops in tumors will provide new therapeutic targets to specifically inhibit invasion and metastasis in primary tumors and metastatic tumors derived from them.

ACKNOWLEDGMENTS

We thank Howard Berg and Benjamin Segall for help in modeling diffusion from the needle tip, and the Analytical Imaging Facility at AECOM.

REFERENCES

1. Hendrix MJ, Seftor EA, Kirschmann DA, Seftor RE. Molecular biology of breast cancer metastasis. Molecular expression of vascular markers by aggressive breast cancer cells. Breast Cancer Res 2000;2:417–22.
2. Liotta LA, Kohn EC. The microenvironment of the tumour-host interface. Nature 2001;411;375–9.
3. Leek RD, Harris AL. Tumor-associated macrophages in breast cancer. J Mammary Gland Biol Neoplasia 2002;7:177–89.
4. O'Sullivan C, Lewis CE. Tumour-associated leucocytes: friends or foes in breast carcinoma. J Pathol 1994;172:229–35.
5. Lin EY, Nguyen AV, Russell RG, Pollard JW. Colony-stimulating factor 1 promotes progression of mammary tumors to malignancy. J Exp Med 2001;193:727–40.
6. Lin EY, Gouon-Evans V, Nguyen AV, Pollard JW. The macrophage growth factor CSF-1 in mammary gland development and tumor progression. J Mammary Gland Biol Neoplasia 2002;7:147–62.
7. Ren Y, Tsui HT, Poon RT, et al. Macrophage migration inhibitory factor: roles in regulating tumor cell migration and expression of angiogenic factors in hepatocellular carcinoma. Int J Cancer 2003;107:22–9.
8. Pollard JW. Tumour-educated macrophages promote tumour progression and metastasis. Nat Rev Cancer 2004;4:71–8.
9. Wyckoff JB, Jones JG, Condeelis JS, Segall JE. A critical step in metastasis: in vivo analysis of intravasation at the primary tumor. Cancer Res 2000;60:2504–11.
10. Farina KL, Wyckoff JB, Rivera J, et al. Cell motility of tumor cells visualized in living intact primary tumors using green fluorescent protein. Cancer Res 1998;58: 2528–32.
11. Wang W, Wyckoff JB, Frohlich VC, et al. Single cell behavior in metastatic primary mammary tumors correlated with gene expression patterns revealed by molecular profiling. Cancer Res 2002;62:6278–88.
12. Calabro A, Orsini B, Renzi D, et al. Expression of epidermal growth factor, transforming growth factor-α and their receptor in the human oesophagus. Histochem J 1997;29:745–58.
13. Peoples GE, Blotnick S, Takahashi K, Freeman MR, Klagsbrun M, Eberlein TJ. T-lymphocytes that infiltrate tumors and atherosclerotic plaques produce heparin-binding epidermal growth factor-like growth factor and basic fibroblast growth factor: a potential pathologic role. Proc Natl Acad Sci USA 1995;92:6547–51.
14. Kume N, Gimbrone MA Jr. Lysophosphatidylcholine transcriptionally induces growth factor gene expression in cultured human endothelial cells. J Clin Invest 1994;93:907–11.
15. Dluz SM, Higashiyama S, Damm D, Abraham JA, Klagsbrun M. Heparin-binding epidermal growth factor-like growth factor expression in cultured fetal human vascular smooth muscle cells. Induction of mRNA levels and secretion of active mitogen. J Biol Chem 1993;268:18330–4.
16. Scagliotti GV, Masiero P, Pozzi E. Biological prognostic factors in non-small cell lung cancer. Lung Cancer 1995;12(Suppl 1):S13–25.
17. Sherwood ER, Lee C. Epidermal growth factor-related peptides and the epidermal growth factor receptor in normal and malignant prostate. World J Urol 1995;13: 290–6.
18. Klijn JG, Look MP, Portengen H, Alexieva-Figusch J, van Putten WL, Foekens JA. The prognostic value of epidermal growth factor receptor (EGF-R) in primary breast cancer: results of a 10 year follow-up study. Breast Cancer Res Treat 1994;29:73–83.
19. Chrysogelos SA, Dickson RB. EGF receptor expression, regulation, and function in breast cancer. Breast Cancer Res Treat 1994;29:29–40.
20. Kaufmann AM, Khazaie K, Wiedemuth M, et al. Expression of epidermal growth factor receptor correlates with metastatic potential of 13762NF rat mammary adenocarcinoma cells. Int J Oncol 1994;4:1149–55.
21. Wyckoff JB, Insel L, Khazaie K, Lichtner RB, Condeelis JS, Segall JE. Suppression of ruffling by the EGF receptor in chemotactic cells. Exp Cell Res 1998;242:100–9.
22. Lichtner RB, Kaufmann AM, Kittmann A, et al. Ligand mediated activation of ectopic EGF receptor promotes matrix protein adhesion and lung colonization of rat mammary adenocarcinoma cells. Oncogene 1995;10:1823–32.
23. Wyckoff JB, Segall JE, Condeelis JS. The collection of the motile population of cells from a living tumor. Cancer Res 2000;60:5401–4.
24. Lin EY, Jones JG, Li P, et al. Progression to malignancy in the polyoma middle T oncoprotein mouse breast cancer model provides a reliable model for human diseases. Am J Pathol 2003;163:2113–26.
25. Guy CT, Cardiff RD, Muller WJ. Induction of mammary tumors by expression of polyomavirus middle T oncogene: a transgenic mouse model for metastatic disease. Mol Cell Biol 1992;12:954–61.
26. Ahmed F, Wyckoff J, Lin EY, et al. GFP expression in the mammary gland for imaging of mammary tumor cells in transgenic mice. Cancer Res 2002;62:7166–9.
27. Faust N, Varas F, Kelly LM, Heck S, Graf T. Insertion of enhanced green fluorescent protein into the lysozyme gene creates mice with green fluorescent granulocytes and macrophages. Blood 2000;96:719–26.
28. Wang W, Wyckoff JB, Wang Y, Bottinger EP, Segall JE, Condeelis JS. Gene expression analysis on small numbers of invasive cells collected by chemotaxis from primary mammary tumors of the mouse. BMC Biotechnol 2003;3:13.
29. Kunkel MW, Hook KE, Howard CT, et al. Inhibition of the epidermal growth factor receptor tyrosine kinase by PD153035 in human A431 tumors in athymic nude mice. Invest New Drugs 1996;13:295–302.
30. Stanley ER. The macrophage colony-stimulating factor, CSF-1. Methods Enzymol 1985;116:564–87.
31. Sudo T, Nishikawa S, Ogawa M, et al. Functional hierarchy of c-kit and c-fms in intramarrow production of CFU-M. Oncogene 1995;11:2469–76.
32. Cantor C, Schimmel PR. Biological Chemistry. San Francisco: W.H. Freeman; 1980. p. 581–6.
33. Berg H. Random Walks in Biology. Princeton, NJ: Princeton University Press; 1983. p. 131–4.
34. Condeelis J, Segall JE. Intravital imaging of cell movement in tumours. Nat Rev Cancer 2003;3:921–30.

35. Wyckoff J, Segall J, Condeelis J. Single cell imaging in animal tumors in vivo In: Spector DL, Goldman RD, editors. Live Cell Imaging: A Laboratory Manual. Cold Spring Harbor, NY: Cold Spring Harbor Laboratories Press; 2004.
36. Austyn JM, Gordon S. F4/80, a monoclonal antibody directed specifically against the mouse macrophage. Eur J Immunol 1981;11:805–15.
37. Bailly M, Yan L, Whitesides GM, Condeelis JS, Segall JE. Regulation of protrusion shape and adhesion to the substratum during chemotactic responses of mammalian carcinoma cells. Exp Cell Res 1998;241:285–99.
38. Wells A. Tumor invasion: role of growth factor-induced cell motility. Adv Cancer Res 2000;78:31–101.
39. Segall JE, Tyerech S, Boselli L, et al. EGF stimulates lamellipod extension in metastatic mammary adenocarcinoma cells by an actin-dependent mechanism. Clin Exp Metastasis 1996;14:61–72.
40. Sapi E, Kacinski BM. The role of CSF-1 in normal and neoplastic breast physiology. Proc Soc Exp Biol Med 1999;220:1–8.
41. Scholl SM, Mosseri V, Tang R, et al. Expression of colony-stimulating factor-1 and its receptor (the protein product of c-fms) in invasive breast tumor cells. Induction of urokinase production via this pathway? Ann NY Acad Sci 1993;698:131–5.
42. Webb SE, Pollard JW, Jones GE. Direct observation and quantification of macrophage chemoattraction to the growth factor CSF-1. J Cell Sci 1996;109(Pt 4):793–803.
43. Ritch PA, Carroll SL, Sontheimer H. Neuregulin-1 enhances motility and migration of human astrocytic glioma cells. J Biol Chem 2003;278:20971–8.
44. Holbro T, Beerli RR, Maurer F, Koziczak M, Barbas CF 3rd, Hynes NE. The ErbB2/ErbB3 heterodimer functions as an oncogenic unit: ErbB2 requires ErbB3 to drive breast tumor cell proliferation. Proc Natl Acad Sci USA 2003;100:8933–8.
45. Ross R, Raines EW, Bowen-Pope DF. The biology of platelet-derived growth factor. Cell 1986;46:155–69.
46. George D. Platelet-derived growth factor receptors: a therapeutic target in solid tumors. Semin Oncol 2001;28:27–33.
47. Krettek A, Ostergren-Lunden G, Fager G, Rosmond C, Bondjers G, Lustig F. Expression of PDGF receptors and ligand-induced migration of partially differentiated human monocyte-derived macrophages. Influence of IFN-γ and TGF-β. Atherosclerosis 2001;156:267–75.
48. Savikko J, von Willebrand E. Coexpression of platelet-derived growth factors AA and BB and their receptors during monocytic differentiation. Transplant Proc 2001;33:2307–8.
49. Hazar B, Paydas S, Zorludemir S, Sahin B, Tuncer I. Prognostic significance of microvessel density and vascular endothelial growth factor (VEGF) expression in non-Hodgkin's lymphoma. Leuk Lymphoma 2003;44:2089–93.
50. Price DJ, Miralem T, Jiang S, Steinberg R, Avraham H. Role of vascular endothelial growth factor in the stimulation of cellular invasion and signaling of breast cancer cells. Cell Growth Differ 2001;12:129–35.
51. Forough R, Lindner L, Partridge C, Jones B, Guy G, Clark G. Elevated 80K-H protein in breast cancer: a role for FGF-1 stimulation of 80K-H. Int J Biol Markers 2003;18:89–98.
52. Byyny RL, Orth DN, Cohen S, Doyne ES. Epidermal growth factor: effects of androgens and adrenergic agents. Endocrinology 1974;95:776–82.
53. Bartocci A, Pollard JW, Stanley ER. Regulation of colony-stimulating factor 1 during pregnancy. J Exp Med 1986;164:956–61.
54. Reith EJ, Ross MH. Atlas of Descriptive Histology, ed 2. New York: Harper & Row, Inc.; 1970. p. 40–4.
55. Li J, Lin ML, Wiepz GJ, Guadarrama AG, Bertics PJ. Integrin-mediated migration of murine B82L fibroblasts is dependent on the expression of an intact epidermal growth factor receptor. J Biol Chem 1999;274:11209–19.
56. Grotendorst GR, Soma Y, Takehara K, Charette M. EGF and TGF-α are potent chemoattractants for endothelial cells and EGF-like peptides are present at sites of tissue regeneration. J Cell Physiol 1989;139:617–23.
57. Morimoto A, Tada K, Nakayama Y, et al. Cooperative roles of hepatocyte growth factor and plasminogen activator in tubular morphogenesis by human microvascular endothelial cells. Jpn J Cancer Res 1994;85:53–62.
58. Cecchini MG, Dominguez MG, Mocci S, et al. Role of colony stimulating factor-1 in the establishment and regulation of tissue macrophages during postnatal development of the mouse. Development 1994;120:1357–72.
59. Wiktor-Jedrzejczak W, Urbanowska E, Aukerman SL, et al. Correction by CSF-1 of defects in the osteopetrotic op/op mouse suggests local, developmental, and humoral requirements for this growth factor. Exp Hematol 1991;19:1049–54.
60. Aharinejad S, Abraham D, Paulus P, et al. Colony-stimulating factor-1 antisense treatment suppresses growth of human tumor xenografts in mice. Cancer Res 2002;62:5317–24.
61. Aharinejad S, Paulus P, Sioud M, et al. Colony-stimulating factor-1 blockade by antisense oligonucleotides and small interfering RNAs suppresses growth of human mammary tumor xenografts in mice. Cancer Res 2004;64:5378–84.
62. Balkwill F, Mantovani A. Inflammation and cancer: back to Virchow? Lancet 2001;357:539–45.
63. Geiger J, Wessels D, Soll DR. Human polymorphonuclear leukocytes respond to waves of chemoattractant, like Dictyostelium. Cell Motil Cytoskeleton 2003;56:27–44.
64. Dormann D, Kim JY, Devreotes PN, Weijer CJ. cAMP receptor affinity controls wave dynamics, geometry and morphogenesis in Dictyostelium. J Cell Sci 2001;114:2513–23.